CHEMISTRY
A EUROPEAN JOURNAL

DOI: 10.1002/chem.200601640

Ionic Interaction as a Powerful Driving Force for the Formation of Heterobidentate Assembly Ligands

Henrik Gulyás, Jordi Benet-Buchholz, Eduardo C. Escudero-Adan, Zoraida Freixa, and Piet W. N. M. van Leeuwen*[a]

Abstract: An ionic interaction has been used for the first time to assemble monophosphane ligands. NMR spectroscopy and X-ray studies show that cationic and anionic triphenylphosphane derivatives form ion pairs and subsequently act as a ligand in various transition-metal complexes. The position of the ionic functional groups allows both *cis* and *trans* coordination of the novel assembly ligand in square-planar transition-metal complexes.

Keywords: chelating ligands · combinatorial chemistry · ion pairs · phosphanes · self-assembly

Introduction

Combinatorial approaches and high-throughput experimentation are of great interest in homogeneous catalysis. A recently developed, and elegant, approach involves using mixtures of monodentate ligands. When considering catalysts in which the active metal species holds two ligands, a mixture of two different monophosphorus compounds, L_a and L_b, may form complexes $[ML_aL_a]$, $[ML_bL_b]$, and $[ML_aL_b]$. If the heterocombination is more active and selective than either of the homocombinations then the new catalytic system (a mixture of $[ML_aL_a]$, $[ML_bL_b]$, and $[ML_aL_b]$) should be more active and selective than the ones that are prepared conventionally from L_a ($[ML_aL_a]$) or L_b ($[ML_bL_b]$). The methodology is extremely powerful because N different monophosphorus ligands lead to the formation of $N \times N$ catalytic systems, which can be tested. This approach has been useful in asymmetric hydrogenation,[1] asymmetric C–C bond formation,[2] and hydroformylation.[3]

Whereas the formation of heterocombinations can be left to mere chance, the idea has emerged that the population of the heterocombinations could be increased by using noncovalent interactions between monophosphorus compounds. This approach uses monodentate ligands that are functionalized with complementary binding sites. Such monophosphorus compounds will form assemblies with one another, and the equilibrium of the complexes described above can be shifted towards the desired heterocomplex. The first examples reported involved the formation and application of heterobidentate ligands assembled by means of Lewis acid–base interactions.[4] The building blocks are monophosphites that have Zn^{II}–porphyrin binding motifs and different monophosphorus ligands with nitrogen donor functionalities. The ligand assemblies have been tested in asymmetric allylic alkylation,[4a,b] hydroformylation,[4b] and asymmetric hydrogenation.[4c] Most recently, complementary hydrogen-bond motifs have been exploited to assemble monophosphorus ligands.[5] It was demonstrated that aminopyridine and isoquinolone functionalities form a pair of strong hydrogen bonds, and the phosphane and phosphonite units that are attached coordinate to the active metal center in a heterobidentate fashion. These ligand systems were used for rhodium-catalyzed hydroformylation of 1-octene,[5a] and also for the asymmetric hydrogenation of several substrates.[5b]

It occurred to us that ionic interactions might be suitable binding motifs for the formation of heterobidentate ligand combinations. Herein, we describe the application of an ionic interaction to assemble triphenylphosphane derivatives, and discuss the influence of the ionic bond on the coordination behavior of phosphanes in comparison with hydrogen bonds.

[a] Dr. H. Gulyás, Dr. J. Benet-Buchholz, E. C. Escudero-Adan, Dr. Z. Freixa, Prof. Dr. P. W. N. M. van Leeuwen
Institute of Chemical Research of Catalonia (ICIQ)
Av. Països Catalans 16, 43007 Tarragona (Spain)
Fax: (+34) 977-920-221
E-mail: pvanleeuwen@iciq.es

Results and Discussion

Ligand $\mathbf{1}^{-}\cdot\mathbf{2}^{+}$ was formed by means of a simple ion-exchange reaction between the monosulfonated triphenylphos-

phane sodium salt (**1**) and 3-(diphenylphosphanyl)aniline hydrochloride (**2**) (Scheme 1). The coordination behavior of ion pair $\mathbf{1}^{-}\cdot\mathbf{2}^{+}$ was tested with various transition-metal com-

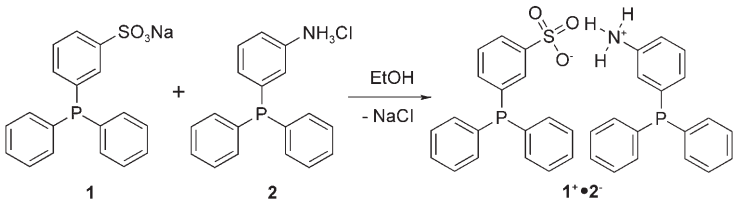

Scheme 1. Synthesis of ligand assembly $\mathbf{1}^{-}\cdot\mathbf{2}^{+}$.

plexes. Other monophosphanes (**3**–**6**) containing functional groups capable of forming hydrogen bonds were also tested to compare the efficiency of different types of noncovalent interactions.

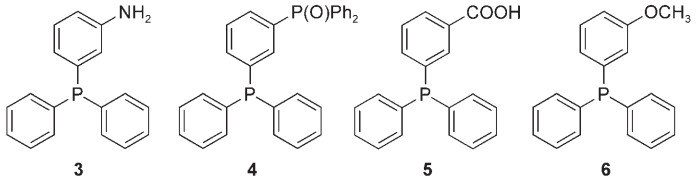

All the monophosphorus ligands that were used are *meta*-substituted triphenylphosphane derivatives. Their structural similarity ensures that they will also have similar binding properties to transition metal centers, and the distribution of the complexes will only be influenced by the interactions of the functional groups.

First, the reactions of phosphanes **1**–**6** with $[PtCl_2(cod)]$ were studied (cod: 1,5-cyclooctadiene). It should be noted that by using this precursor, under the chosen reaction conditions, each of the monophosphanes forms *cis*-$[PtCl_2L_2]$ as the major product in which L: phosphane (Table 1; Figure 2A (see below)). These results suggest that *cis* geometry of the platinum complexes is not necessarily due to attractive ligand–ligand interactions.[6]

The statistical distribution of *cis*-$[PtCl_2L_aL_b]$, *cis*-$[PtCl_2(L_a)_2]$, and *cis*-$[PtCl_2(L_b)_2]$ has been modeled by using a mixture of anisyldiphenylphosphane (**6**) and triphenylphosphane (tpp). No significant attractive interactions were expected, and accordingly, *cis*-$[Pt(\mathbf{6})Cl_2(tpp)]$, *cis*-$[Pt(\mathbf{6})_2Cl_2]$, and *cis*-$[PtCl_2(tpp)_2]$ were observed by means of $^{31}P\{^1H\}$ NMR spectroscopy in a ratio of 2:1:1 (Table 2). For **3**/**5**, **4**/**5**, and **2**/**4** ligand mixtures, the formation of $COOH\cdots NH_2$, $COOH\cdots O{=}P$, and $NH_3^{+}\cdots O{=}P$ hydrogen bonds might have been anticipated,[7] however, under the conditions used no increase in heterocombinations was achieved. An interesting phenomenon was observed over the course of the reaction of $[PtCl_2(cod)]$ with a 1:1 mixture of *m*-(diphenylphosphanyl)aniline (**3**) and its hydrochloride (**2**). The $^{31}P\{^1H\}$ NMR spectrum displays only one singlet at $\delta = 16.7$ ppm with a coupling constant of $^1J(Pt,P) = 3684$ Hz. These NMR characteristics suggest that a fast intermolecular–intramolecular proton exchange among the nitrogen atoms renders the two *cis*-oriented phosphanes equivalent on the NMR timescale. An X-ray study of the crystals obtained from the reaction mixture confirms the formation of

Table 1. Reaction of triphenylphosphane derivatives and $[PtCl_2(cod)]$.[a]

Phosphane	Solvents	Products[b]	^{31}P NMR [ppm] (J in Hz)	Product distribution [%]
1	CD_3OD	*cis*-$[PtCl_2L_2]$, $[PtClL_3]$, *cis*-$[Pt(CD_3OD)_2L_2]$	17.07 (s, $J(Pt,P) = 3702$); 15.40 (t, $J(P,P) = 19.8$, $J(Pt,P) = 3664$, 1P), 25.91 (d, $J(P,P) = 19.8$, $J(Pt,P) = 2511$, 2P); 22.92 (s, $J(Pt,P) = 3123$)	78, 16, 6
2	$CDCl_3$	*cis*-$[PtCl_2L_2]$	17.18 (s, $J(Pt,P) = 3696$)	100
3	$CDCl_3$	*cis*-$[PtCl_2L_2]$	17.56 (s, $J(Pt,P) = 3694$)	100
4	$[D_7]DMF$	*cis*-$[PtCl_2L_2]$	18.00 (s, $J(Pt,P) = 3662$, P^{III}), 27.71 (s, P^{V})	100
5	$CDCl_3/CD_3OD$[c]	*cis*-$[PtCl_2L_2]$, *trans*-$[PtCl_2L_2]$	17.14 (s, $J(Pt,P) = 3684$), 23.80 (s, $J(Pt,P) = 2640$)	95, 5
6	$CDCl_3$	*cis*-$[PtCl_2L_2]$	17.72 (s, $J(Pt,P) = 3674$)	100

[a] $[PtCl_2(cod)]$ (0.04 mmol) and tpp derivative (0.084 mmol) were transferred to a Schlenk tube before the solvent was added, and the mixture was stirred for 10–30 min. [b] L = phosphane. [c] 5:1 ratio.

Table 2. Attempts at the formation of assemblies of tpp derivatives by using hydrogen bonds.[a]

Phosphanes	Functional groups	Solvents (quantities in mL)	Products	Distribution [%]
tpp, **6**[b]	–, OCH_3	$[CDCl_3]/\{DMF\}$ (1:1)	*cis*-$[PtCl_2L_aL_b]$, *cis*-$[PtCl_2(L_a)_2]$, *cis*-$[PtCl_2(P_b)_2]$	50, 25, 25
3, **5**[b]	NH_2, COOH	$[CDCl_3]/\{DMF\}$ (1:1)	*cis*-$[PtCl_2L_aL_b]$, *cis*-$[PtCl_2(L_a)_2]$, *cis*-$[PtCl_2(L_b)_2]$	50, 25, 25
3, **5**[c]	NH_2, COOH	$CDCl_3$/THF (1:0.1)	*cis*-$[PtCl_2L_aL_b]$, *cis*-$[PtCl_2(L_a)_2]$, *cis*-$[PtCl_2(L_b)_2]$	50, 25, 25
4, **5**[b]	P=O, COOH	$[CDCl_3]/\{DMF\}$ (1:1)	*cis*-$[PtCl_2L_aL_b]$, *cis*-$[PtCl_2(L_a)_2]$, *cis*-$[PtCl_2(L_b)_2]$	50, 25, 25
4, **5**[c]	P=O, COOH	$[CDCl_3]$ (1)	*cis*-$[PtCl_2L_aL_b]$, *cis*-$[PtCl_2(L_a)_2]$, *cis*-$[PtCl_2(L_b)_2]$	50, 25, 25
2, **4**[b]	P=O, NH_3^{+}	$[CDCl_3]/\{DMF\}$ (1:1)	*cis*-$[PtCl_2L_aL_b]$, *cis*-$[PtCl_2(L_a)_2]$, *cis*-$[PtCl_2(L_b)_2]$	50, 25, 25
2, **3**[b]	NH_2, NH_3^{+}	$[CDCl_3]/\{DMF\}$ (1:1)	*cis*-$[PtCl_2L_aL_b]$[d]	100

[a] $[PtCl_2(cod)]$ (0.04 mmol) and equimolar amounts of both phosphanes (0.042 mmol). [b] The solution of the ligand mixture (solvent in []) was added to the solution of the precursor (solvent in {}), and the reaction mixture was stirred for 10–30 min. [c] The solution of the ligand mixture was added to the solid precursor, and the reaction mixture was stirred for 10–30 min. [d] The two coordinated phosphanes are equivalent on the NMR timescale.

cis-[Pt(**2**)(**3**)Cl_2], although in the solid state $NH_3^+\cdots Cl^-$ interactions are observed instead of $NH_3^+\cdots NH_2$ hydrogen bonds (Figure 1).

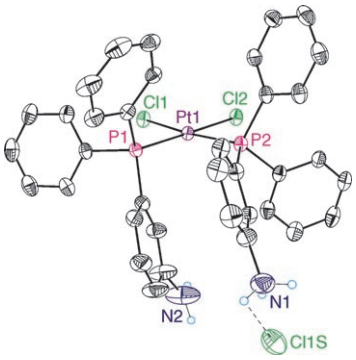

Figure 1. X-ray structure of *cis*-[Pt(**2**)(**3**)Cl_2].[8]

In contrast to the mixtures of tpp derivatives that are only capable of forming hydrogen bonds, the phosphane ion pair **1**$^-$·**2**$^+$ did increase the formation of heterocomplex *cis*-[Pt(**1**$^-$·**2**$^+$)Cl_2] to as much as 97% (Table 3).[9] The byproduct is the ion pair formed from the homocombinations of *cis*-[Pt(**1**$^-$)$_2Cl_2$]·*cis*-[Pt(**2**$^+$)$_2Cl_2$] (**1**$^-$: **1**–Na^+; **2**$^+$: **2**–Cl^-);[10] its relative proportion depends on the solvents used, the concentration of the reaction mixtures, and the way that the complexes are made (Table 3). It is particularly remarkable that the ion pair **1**$^-$·**2**$^+$ formed 77% of the heterocombination, even in strongly polar, protic solvents, such as a 1:1 mixture of MeOH/DMF (Table 3, entry 8). The X-ray structure confirms the *cis* coordination and the presence of the expected $NH_3^+\cdots{}^-O_3S$ ionic bond (Figure 2B). Again it is important to note that this ionic bond is not necessarily the cause of the *cis* coordination. Both the NMR data summarized in Table 1, and the X-ray structure of *cis*-[Pt(**6**)$_2Cl_2$] (Figure 2A) reveal that triarylphosphanes lacking complementary functional groups can form *cis*-[$PtCl_2L_2$] complexes with high selectivity.[6]

To survey the coordination properties of the ligand assembly **1**$^-$·**2**$^+$, [Pd(CH_3)Cl(cod)] was chosen as a precursor. The

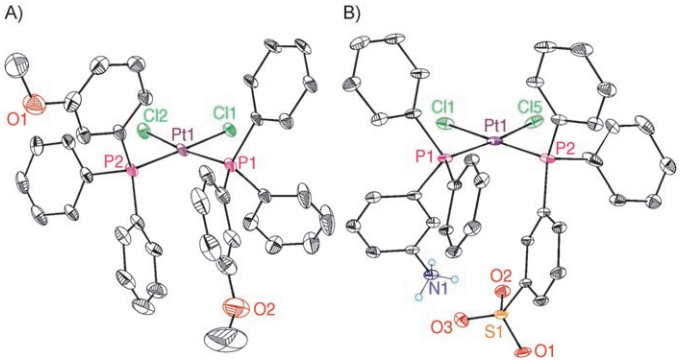

Figure 2. X-ray structure of A) *cis*-[Pt(**6**)$_2Cl_2$] and B) *cis*-[Pt(**1**$^-$·**2**$^+$)Cl_2].[11]

reaction of phosphanes with this transition-metal complex is greatly influenced by their structure. Bisphosphanes with a small bite angle give *cis* complexes, whereas *trans*-spanning bis- and monophosphanes favor the *trans*-coordination mode. The different coordination modes result in rather distinctive $^{31}P\{^1H\}$ NMR spectra. The reaction of **1**$^-$·**2**$^+$ and [Pd(CH_3)Cl(cod)] could be studied in relatively apolar halogenated hydrocarbon solvents (CD_2Cl_2 and $CDCl_3$) without the addition of polar cosolvents. The chemical shifts of the coordinated phosphanes in the $^{31}P\{^1H\}$ NMR spectrum are very similar, which results in a single broad resonance at $\delta =$ 34.4 ppm. This pattern excludes the possibility of *cis* coordination, and the *trans* position of the phosphanes was proven by means of X-ray studies (Figure 3B). Most interestingly, the structure reveals that in this coordination mode the ionic bond can be as efficient as in the case of *cis* coordination.[12] The conformation of the ionically assembled ligand is quite different from that of monophosphanes that lack complementary binding motifs (Figure 3A), and rather resembles the coordination of *trans*-spanning bisphosphanes.

Finally, we studied the reaction of **1**$^-$·**2**$^+$ and [{Rh(CO)$_2$Cl}$_2$]. To the best of our knowledge, the coordination behavior of bisphosphanes assembled by using noncovalent interactions has not yet been tested with dimeric precursors. Despite the presumably more complex reaction mechanism, a single product was observed in the $^{31}P\{^1H\}$ NMR spectrum (Figure 4A), in which **1**$^-$·**2**$^+$ is coor-

Table 3. Reactions of ionic assembly **1**$^-$·**2**$^+$ and [$PtCl_2$(cod)].[a]

Method[b]	Solvents (quantities in mL)	Products[c]	Distribution [%]
A	$CDCl_3/CD_3OD$ (1:0.2)	*cis*-[Pt(**1**$^-$·**2**$^+$)Cl_2], *cis*-[Pt(**1**$^-$)$_2Cl_2$]·*cis*-[Pt(**2**$^+$)$_2Cl_2$]	83, 17[d]
A	[D_7]DMF (1)	*cis*-[Pt(**1**$^-$·**2**$^+$)Cl_2], *cis*-[Pt(**1**$^-$)$_2Cl_2$]·*cis*-[Pt(**2**$^+$)$_2Cl_2$]	80, 10, 10
A	THF/[D_7]DMF (9:1)	*cis*-[Pt(**1**$^-$·**2**$^+$)Cl_2], *cis*-[Pt(**1**$^-$)$_2Cl_2$]·*cis*-[Pt(**2**$^+$)$_2Cl_2$]	97, 1.5, 1.5
B	[$CDCl_3$]/{$CDCl_3/CD_3OD$} (0.5:0.5:0.2)	*cis*-[Pt(**1**$^-$·**2**$^+$)Cl_2], *cis*-[Pt(**1**$^-$)$_2Cl_2$]·*cis*-[Pt(**2**$^+$)$_2Cl_2$]	85, 15[d]
B	[DMF]/{DMF} (0.5:0.5)	*cis*-[Pt(**1**$^-$·**2**$^+$)Cl_2], *cis*-[Pt(**1**$^-$)$_2Cl_2$]·*cis*-[Pt(**2**$^+$)$_2Cl_2$]	80, 10, 10
B	[DMF]/{DMF} (1:1)	*cis*-[Pt(**1**$^-$·**2**$^+$)Cl_2], *cis*-[Pt(**1**$^-$)$_2Cl_2$]·*cis*-[Pt(**2**$^+$)$_2Cl_2$]	83, 8.5, 8.5
B	[$CDCl_3$]/{DMF} (1:1)	*cis*-[Pt(**1**$^-$·**2**$^+$)Cl_2], *cis*-[Pt(**1**$^-$)$_2Cl_2$]·*cis*-[Pt(**2**$^+$)$_2Cl_2$]	85, 7.5, 7.5
B	[CD_3OD]/{DMF} (1:1)	*cis*-[Pt(**1**$^-$·**2**$^+$)Cl_2], *cis*-[Pt(**1**$^-$)$_2Cl_2$]·*cis*-[Pt(**2**$^+$)$_2Cl_2$]	77, 11.5, 11.5
B	[$CHCl_3/CDCl_3$]/{$CHCl_3$/DMF} (4:1:4:1)	*cis*-[Pt(**1**$^-$·**2**$^+$)Cl_2], *cis*-[Pt(**1**$^-$)$_2Cl_2$]·*cis*-[Pt(**2**$^+$)$_2Cl_2$]	90, 5, 5

[a] [$PtCl_2$(cod)] (0.04 mmol) and **1**$^-$·**2**$^+$ (0.042 mmol). [b] Method A: The precursor and the assembly ligand were transferred to a Schlenk tube before the solvent was added, and the mixture was stirred for 10–30 min. Method B: The solution of assembly ligand **1**$^-$·**2**$^+$ (solvent in []) was added to the solution of the precursor (solvent in {}), and the reaction mixture was stirred for 10–30 min. [c] For representative $^{31}P\{^1H\}$ NMR data see refs. [9] and [10]. [d] The resonances of the anionic and cationic complexes overlap.

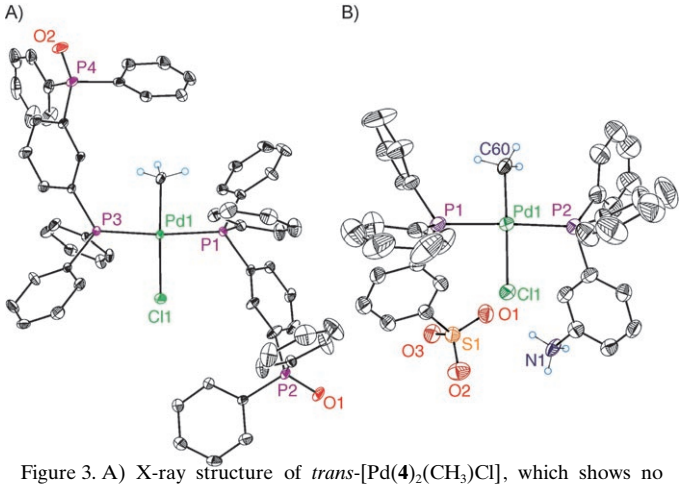

Figure 3. A) X-ray structure of *trans*-[Pd(**4**)$_2$(CH$_3$)Cl], which shows no significant interaction between the functionalized tpp derivatives; B) X-ray structure of *trans*-[Pd(**1**$^-$·**2**$^+$)(CH$_3$)Cl], ionic assembly **1**$^-$·**2**$^+$ acts as a *trans*-spanning assembly ligand, which maintains the ionic interaction in the *trans* position.[13]

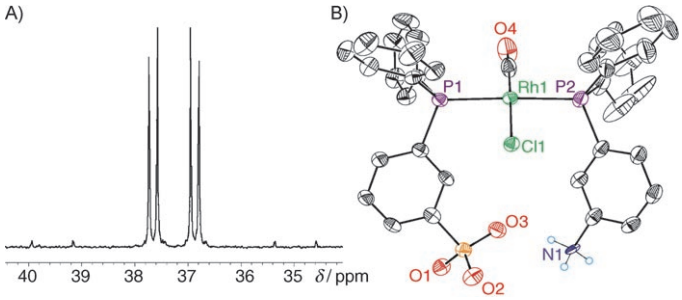

Figure 4. A) The ^{31}P{^{1}H} NMR spectrum and B) the X-ray structure of *trans*-[Rh(**1**$^-$·**2**$^+$)(CO)Cl].[14]

dinated as a heterobidentate ligand. The characteristics of the strongly distorted ABX spin system (δ = 36.1 ppm, ^1J(Rh,P) = 125 Hz, ^2J(P,P) = 357 Hz; δ = 38.7 ppm, ^1J(Rh,P) = 125 Hz, ^2J(P,P) = 357 Hz) indicate the *trans* position of the two phosphorus atoms. The X-ray structure of [Rh(**1**$^-$·**2**$^+$)(CO)Cl] (Figure 4B) is very similar to that of palladium complex [Pd(**1**$^-$·**2**$^+$)(CH$_3$)Cl], which confirms that the *trans* coordination mode allows the formation of a strong $NH_3^+\cdots{}^-O_3S$ electrostatic interaction.[12]

Conclusion

In summary, we have used an ionic bond as the driving force for the formation of a heterobidentate phosphane for the first time. A number of test reactions have shown that the cationic and anionic monodentate phosphorus ligands form an ion pair even in strongly polar, protic media. The ligand design, that is the position of the ionic functional groups, allows both *cis* and *trans* coordination of **1**$^-$·**2**$^+$ in square-planar transition-metal complexes. It remains to be seen how this novel supramolecular strategy can be applied in homogeneous catalytic reactions.

Experimental Section

General remarks: All manipulations were carried out under argon by using Schlenk techniques. Solvents were purified, dried, and deoxygenated by using standard methods. Tpp, fuming sulfuric acid, {[3-*N*,*N*-bis(trimethylsilyl)amino]phenyl}magnesium chloride, chlorodiphenylphosphane, 3-bromoanisole, magnesium turnings, solution of HCl in methanol, [PtCl$_2$(cod)], and [{Rh(CO)$_2$Cl}$_2$] were purchased from Sigma-Aldrich and used as received. [Pd(CH$_3$)Cl(cod)][15] and **5**[16] were prepared according to literature procedures. Diphenylphosphane,[17] **1**,[18] **2**,[19], **3**,[19] and **6**[20] were prepared based on modified literature methods (see below). ^{31}P{^{1}H}, ^{1}H, and ^{13}C{^{1}H} NMR spectra were recorded by using a Bruker ATM-400 spectrometer operating at 161.98, 400.13, and 100.61 MHz, respectively. Mass spectra were recorded by using a Waters LCT Premier spectrometer.

Sodium 3-(diphenylphosphanyl)benzenesulfonate (1): PPh$_3$ (10 g, 38.2 mmol) was added portionwise over 90 min to fuming sulfuric acid (20 mL, 30 wt %) under argon, while the flask was cooled in an ice bath. The homogeneous reaction mixture was heated at 93 °C for 2 h. The acidic solution was quenched by the addition of ice (40 g), and it was diluted with deoxygenated water (100 mL). Adjusting the pH of the reaction mixture to 6–7 by using an aqueous NaOH solution (30 %) gave a milky suspension. The precipitate was filtered and dried in vacuo. The crude product was recrystallized twice from deoxygenated water to give colorless microcrystals (4.16 g, 29 %). ^{1}H NMR (CD$_3$OD): δ = 7.24–7.36 (m, 12 H; Ph and sulfonated), 7.40 (broad pseudo t, $J \approx 7$–8 Hz, 1 H; sulfonated), 7.84 (br d, $J \approx 7.6$ Hz, 1 H; sulfonated), 7.87 ppm (br d, $J \approx 7.5$ Hz, 1 H; sulfonated); ^{13}C{^{1}H} NMR (CD$_3$OD): δ = 127.5 (s; sulfonated), 129.6 (d, ^1J(P,C) = 6.1 Hz; sulfonated), 129.7 (d, ^3J(P,C) = 7.2 Hz; *m*-phenyl), 130.1 (s, *p*-phenyl), 132.0 (d, J(P,C) = 22.9 Hz; sulfonated), 134.8 (d, ^2J(P,C) = 19.1 Hz; *o*-phenyl), 136.3 (d, J(P,C) = 18.2 Hz; sulfonated), 138.0 (d, J(P,C) = 10.8 Hz; *ipso*-phenyl), 139.7 (d, J(P,C) = 14.6 Hz; sulfonated), 146.6 ppm (d, J(P,C) = 6.2 Hz; sulfonated); ^{31}P{^{1}H} NMR (CD$_3$OD): δ = −2.0 ppm (s); ESMS: *m*/*z*: 341.0 [*M*−Na$^+$]$^-$; elemental analysis calcd (%) for C$_{18}$H$_{14}$NaO$_4$PS·H$_2$O: C 56.54, H 4.22, S 8.39; found: C 56.01, H 4.22, S 7.94.

3-(Diphenylphosphanyl)aniline (3): PPh$_2$Cl (17.95 mL, 100 mmol) was added dropwise over 15 min to 1 M solution of {[3-*N*,*N*-bis(trimethylsilyl)amino]phenyl}magnesium chloride in THF (100 mL, 100 mmol) while the reaction flask was cooled in an ice bath. The PPh$_2$Cl residue was rinsed into the reaction mixture from the dropping funnel with THF (30 mL). The reaction mixture was stirred overnight. The solvent was removed in vacuo and the solid residue was extracted with Et$_2$O (3 × 300 mL). The crude diphenyl{[*N*,*N*-bis(trimethylsilyl)amino]phenyl}phosphane was isolated by removing volatile compounds in vacuo. The crude product was dissolved in MeOH (320 mL) and the solution was left at reflux for 12 h. The solution was concentrated in vacuo to precipitate the product as a white microcrystalline solid (16.14 g). Further product (4.57 g) was obtained from the mother liquor after the solvent was removed and the residue was recrystallized from a minimum amount of hot methanol, to give an overall yield of 75 % (20.71 g). ^{1}H NMR (CDCl$_3$): δ = 3.6 (br s, 2 H), 6.61–7.74 ppm (m, 14 H); ^{13}C{^{1}H} NMR (CDCl$_3$): δ = 115.6 (s; C$_6$H$_4$NH$_2$), 120.1 (d, J(C,P) = 20.5 Hz; C$_6$H$_4$NH$_2$), 124.1 (d, J(C,P) = 19.8 Hz; C$_6$H$_4$NH$_2$), 128.5 (d, J(C,P) = 6.6 Hz; Ph), 128.7 (s; Ph), 129.4 (d, J(C,P) = 8.1 Hz; C$_6$H$_4$NH$_2$), 133.8 (d, J(C,P) = 19.8 Hz; Ph), 137.3 (d, J(C,P) = 11.0 Hz; Ph), 138.1 (d, J(C,P) = 9.5 Hz; C$_6$H$_4$NH$_2$), 146.9 ppm (br d, J(C,P) = 8.1 Hz; C$_6$H$_4$NH$_2$); ^{31}P{^{1}H} NMR (CDCl$_3$): δ = −3.1 ppm (s); ESMS: *m*/*z*: 278.1 [*M*+H$^+$]$^+$; elemental analysis calcd (%) for C$_{18}$H$_{16}$NP: C 77.96, H 5.82, N 5.05; found: C 76.79, H 6.27, N 5.12.

3-(Diphenylphosphanyl)aniline hydrochloride (2): A solution of 1.25 M HCl in MeOH (8.0 mL, 10 mmol) was slowly added to a solution of *m*-aminophenyldiphenylphosphane (2.77 g, 10 mmol) in CH$_2$Cl$_2$ (20 mL) and stirred for 1 h at room temperature. The solvents were removed in

vacuo to give a white solid residue, which was suspended in Et_2O (80 mL) and isolated by means of filtration. The product was washed with further Et_2O (20 mL) and it was dried under vacuum (2.31 g, 73%). ^1H NMR ($CDCl_3$): $\delta = 7.08–7.41$ (m, 14H), 10.20 ppm (br s, 3H; NH_3^+); $^{13}C\{^1H\}$ NMR ($CDCl_3$): $\delta = 123.3$ (s), 127.9 (J(C,P) = 25.6 Hz), 128.8 (J(C,P) = 7.3 Hz), 129.2 (s), 130.0 (J(C,P) = 5.1 Hz), 130.4 (J(C,P) = 9.5 Hz), 133.8 (J(C,P) = 19.8 Hz), 135.9 (J(C,P) = 10.2 Hz), 141.0 ppm (J(C,P) = 16.1 Hz); $^{31}P\{^1H\}$ NMR ($CDCl_3$): $\delta = -2.17$ ppm; ESMS: m/z: 278.1 $[M-Cl^-]^+$; elemental analysis calcd (%) for $C_{18}H_{17}ClNP$: C 68.90, H 5.46, N 4.46; found: C 68.66, H 5.68, N 4.51.

3-(Diphenylphosphanyl)(triphenylphosphane oxide) (4): BuLi (6 mL, 2.5 M in hexane, 15 mmol) was slowly added over a period of 10 min to (3-bromophenyl)diphenylphosphane (5.12 g, 15 mmol) dissolved in THF (120 mL) at an external temperature of −85 to −80 °C. The dark red solution was stirred at this temperature for 30 min before $MgBr_2 \cdot Et_2O$ (4.45 g, 17.3 mmol) was added in one portion. The reaction mixture was allowed to reach −10 °C over a period of 3.5 h. This solution was added to $Ph_2P(O)Cl$ (2.9 mL, 15 mmol) dissolved in THF (35 mL) while the flask was cooled with an ice bath. The reaction mixture was stirred overnight and the inorganic salts precipitated from the solution. The reaction mixture was then filtered through a pad of alumina, was concentrated to half of its original volume, and the reaction mixture was quenched with deoxygenated water (100 mL). Diethyl ether (60 mL) was added, and the organic phase was separated. The aqueous phase was washed with EtOAc (2×30 mL), the combined organic phase was washed with water (pH 7), and it was dried over $MgSO_4$. The solvent was removed to give a waxy residue. The crude product contained considerable amounts of PPh_3, and it was purified by means of column chromatography (neutral Al_2O_3; toluene→Et_2O/THF(8:1)→THF). Removal of the solvent resulted in a colorless, glassy material (2.75 g), which was dissolved in Et_2O and subsequently precipitated by adding hexane to give the product as an off-white solid (1.32 g, 19%). ^1H NMR ($CDCl_3$): $\delta = 7.19–7.27$ (m, 10H), 7.28–7.64 (m, 13H), 7.79 ppm (m, 1H); $^{31}P\{^1H\}$ NMR ($CDCl_3$): $\delta = -2.39$ (s, P^{III}), 31.66 ppm (s, P^V); ESMS (%): m/z: 463.1 (40) $[M+H^+]^+$, 485.1 (100) $[M^++Na^+]$; elemental analysis calcd (%) for $C_{30}H_{24}OP_2$: C 77.91, H 5.23; found: C 78.00, H 5.76.

(3-Methoxyphenyl)(diphenyl)phosphane (6): Ph_2PCl (18.75 g, 85 mmol) was added dropwise to a solution of 3-anisylmagnesium bromide in THF (prepared from 3-bromoanisole (18.7 g, 100 mmol) in THF (100 mL) and an excess of magnesium (3.16 g, 130 mmol), while the flask was chilled with crushed ice. The Ph_2PCl residue was rinsed from the dropping funnel into the reaction mixture with THF (10 mL). The ice bath was removed and the reaction mixture was stirred overnight at room temperature. The organic layer was separated from the inorganic salts by using a cannula, and it was concentrated to about a third of the original volume. It was quenched with 10% aqueous NH_4Cl solution (10 g), diluted with Et_2O (80 mL) and THF (20 mL), and then extracted with water (2× 40 mL). The second aqueous extract was washed with a THF/Et_2O (1:1) mixture (20 mL). The combined organic phase was dried over $MgSO_4$. Removal of the solvent resulted in a yellowish oil, which was purified by means of distillation (165–176 °C, 0.20 mbar) to give a colorless, viscous liquid (21.20 g, 85%). After several weeks in the fridge, the product had not crystallized, however, it could be crystallized in the following manner: Some of the product (12.06 g) was dissolved in hot ethanol. The mixture, which was a clear solution at room temperature, was cooled to −20 °C, and it was slowly concentrated in vacuo. The product precipitated as a white microcrystalline solid, which was isolated by decanting the mother liquor by using a cannula (11.60 g). M.p. 55–58 °C; ^1H NMR ($CDCl_3$): $\delta = 3.62$ (s, 3H; OCH_3), 6.73–6.83 (m, 3H; $C_6H_4OCH_3$), 7.17 (m, 1H; $C_6H_4OCH_3$), 7.20–7.23 ppm (m, 10H; Ph); $^{13}C\{^1H\}$ NMR ($CDCl_3$): $\delta = 55.3$ (s; OCH_3), 114.5 (s; anisyl), 119.2 (d, J(C,P) = 21.2 Hz; anisyl), 126.2 (d, J(C,P) = 19.0 Hz; anisyl), 128.7 (d, ^3J(P,C) = 7.3 Hz; *m*-phenyl), 128.9 (s; *p*-phenyl), 129.7 (d, J(C,P) = 7.3 Hz; anisyl), 133.9 (d, ^2J(P,C) = 19.0 Hz; *o*-phenyl), 137.2 (d, J(P,C) = 11.0 Hz; *ipso*-phenyl), 138.9 (d, J(C,P) = 11.0 Hz; anisyl), 159.7 ppm (d, J(C,P) = 8.8 Hz; anisyl); $^{31}P\{^1H\}$ NMR ($CDCl_3$): $\delta = -1.5$ ppm (s); ESMS: m/z: 293.1 $[M+H^+]^+$; elemental analysis calcd (%) for $C_{19}H_{17}OP$: C 78.07, H 5.86; found: C 78.06, H 6.36.

Diphenylphosphane: THF (300 mL) was added slowly to a stirred mixture of triphenylphosphane (52.46 g, 200 mmol) and lithium granules (5.55 g, 800 mmol). The reaction started immediately and the solution turned dark red. The reaction mixture was stirred for 27 h before a ^{31}P NMR spectrum of the solution indicated that full conversion, without any side reactions, had occurred. An excess of water (5 mL) was slowly added to the reaction mixture while the flask was cooled with an ice bath. The reaction mixture was then diluted with Et_2O (100 mL), and washed with 13.4 wt% aqueous NH_4Cl solution (2×100 g, 2×250 mmol) and water (2×50 mL). The organic phase was dried overnight over $MgSO_4$ before the solution was filtered and the solvents were removed in vacuo. The crude product was purified by means of vacuum distillation (1.7–1.9 mbar, 130–160 °C (oil bath)) to give a colorless liquid (27.35 g, 74%). ^1H NMR ($CDCl_3$): $\delta = 5.22$ (d, J(P,H) = 218 Hz, 1H; P-H), 7.22–7.50 ppm (m, 10H; Ph); $^{13}C\{^1H\}$ NMR ($CDCl_3$): $\delta = 128.6$ (s; *para*), 128.8 (d, J(C,P) = 6.6 Hz; *meta*), 134.2 (d, J(C,P) = 16.8 Hz; *ortho*), 134.9 ppm (d, J(C,P) = 10.2 Hz; *ipso*); $^{31}P\{^1H\}$ NMR ($CDCl_3$): $\delta = -37.12$ (s), −37.19 ppm (doublet of quintets, ^1J(P,H) = 218 Hz, ^3J(P,H) = 7.4 Hz).

3-(Diphenylphosphanyl)anilinium-3-(diphenylphosphanyl)benzenesulfonate ($1^-\cdot 2^+$): Compounds **1** (764 mg, 2 mmol) and **2** (628 mg, 2 mmol) were stirred in EtOH (10 mL) for one hour before CH_2Cl_2 (5 mL) was added, and the reaction mixture was left to stand until the precipitate settled. The solution phase was carefully decanted through a fine-porosity glass sinter by using a metal cannula. The solvents were removed in vacuo and the white solid residue was redissolved in CH_2Cl_2 (15 mL). The opaque solution was left to stand for a few hours until the precipitate had settled, and the solution phase (still slightly iridescent) was decanted. The solvent was evaporated and the product was dried in vacuo to give a white solid (1238 mg, quantitative). ^1H NMR ($CDCl_3$): $\delta = 6.98–7.18$ (m, 4H), 7.18–7.32 (m, 21H), 7.37 (br d, J = 7.0 Hz), 7.50 (br d, J = 7.6 Hz), 7.82 (br d, J = 8.2 Hz), 9.70 ppm (br s, 3H; NH_3^+); $^{13}C\{^1H\}$ NMR ($CDCl_3$): $\delta = 123.5$ (s), 126.4 (s), 128.0 (J(C,P) = 24.2 Hz), 128.6 (^3J(C,P) = 7.3 Hz; *m*-phenyl), 128.6 (d, ^3J(P,C) = 7.3 Hz; *m*-phenyl), 128.9 (s; *p*-phenyl), 129.0 (s; *p*-phenyl), 129.7 (d, J(C,P) = 5.1 Hz), 131.3 (d, J(C,P) = 29.3 Hz), 131.4 (d, J(C,P) = 8.1 Hz), 133.3 (d, J(C,P) = 15.4 Hz), 133.7 (^2J(C,P) = 19.8 Hz; *o*-phenyl), 133.8 (^2J(C,P) = 19.8 Hz; *o*-phenyl), 135.4 (d, J(C,P) = 11.0 Hz), 136.2 (d, ^1J(C,P) = 11.0 Hz; *ipso*-phenyl), 136.2 (d, ^1J(C,P) = 11.0 Hz; *ipso*-phenyl), 136.6 (d, ^1J(C,P) = 11.0 Hz; *ipso*-phenyl), 138.1 (d, J(C,P) = 14.6 Hz), 140.1 (d, J(C,P) = 14.6 Hz), 143.3 ppm (d, J(C,P) = 8.8 Hz); $^{31}P\{^1H\}$ NMR ($CDCl_3$): $\delta = -2.35$ (s), −2.20 ppm (s); $ESMS^+$: m/z: 278.1 $[M-$(diphenylphosphanyl)benzenesulfonate$]^+$; $ESMS^-$: m/z: 341.0 $[M-$(diphenylphosphanyl)anilinium$]^-$; elemental analysis calcd (%) for $C_{36}H_{31}NO_3P_2$: C 69.78, H 5.04, N 2.26, S 5.17; found: C 69.17, H 5.18, N 2.28, S 4.60.

Crystallization techniques and X-ray studies

General: CCDC 622934–622939 contain the supplementary crystallographic data for this paper. These data can be obtained free of charge from the Cambridge Crystallographic Data Centre via www.ccdc.cam.ac.uk/data_request/cif.

cis-*[Pt(**2**)(**3**)Cl$_2$]*: Compounds **2** (11.9 mg, 0.042 mmol) and **3** (11.6 mg, 0.042 mmol) were dissolved in $CDCl_3$ (1 mL). The phosphane solution was added to $[PtCl_2(PhCN)_2]$ (15 mg) dissolved in DMF (1 mL). Crystallization of the product was initiated by layering Et_2O on the top of the solution. $^{31}P\{^1H\}$ NMR ($CDCl_3$/DMF): $\delta = -16.75$ ppm (s, J(Pt,P) = 3682 Hz).

cis-*[Pt(**6**)$_2$Cl$_2$]*: $[PtCl_2(cod)]$ (15.0 mg, 0.04 mmol) and **6** (24.6 mg, 0.084 mmol) were stirred in $CDCl_3$ for 45 min to form a homogeneous, colorless solution. Crystallization of the product was initiated by layering Et_2O on the top of the solution. $^{31}P\{^1H\}$ NMR ($CDCl_3$): $\delta = -17.72$ ppm (s, J(Pt,P) = 3674 Hz).

cis-*[Pt(**1**$^-\cdot$**2**$^+$)Cl$_2$]*: Several experiments were carried out to determine the structure of this compound. The crystals are sensitive and tend to lose solvent molecules quickly, which results in the collapse of the crystal. The best quality crystals were obtained in the following manner: Ionic assembly $\mathbf{1}^-\cdot\mathbf{2}^+$ (26 mg, 0.042 mmol) and $[PtCl_2(cod)]$ (15.0 mg, 0.04 mmol) were stirred in CH_3CN for a few seconds. DMF (1 mL) was added within a minute and the reaction mixture was stirred for an hour to obtain a ho-

mogeneous solution. The next day colorless crystals of *cis*-[Pt(**1**$^{-}$·**2**$^{+}$)Cl_2] had deposited on the wall of the vial.

trans-*[Pd(**4**)$_2$(CH$_3$)Cl]*: [Pd(CH_3)Cl(cod)] (10.6 mg, 0.04 mmol) and **4** (38.8 mg, 0.084 mmol) were dissolved in CD_2Cl_2 (1 mL). Crystallization of the product was initiated by layering pentane on the top of the solution. $^{31}P\{^1H\}$ NMR (CD_2Cl_2): $\delta = 29.93$ (s, 1P), 33.89 ppm (s, 1P).

trans-*[Pd(**1**$^{-}$·**2**$^{+}$)(CH$_3$)Cl]*: Ionic assembly **1**$^{-}$·**2**$^{+}$ (26 mg, 0.042 mmol) and [Pd(CH_3)Cl(cod)] (10.6 mg, 0.04 mmol) were dissolved in $CDCl_3$ (1 mL). Layering Et_2O on the top of the solution initiated crystallization of the product within a few hours. $^{31}P\{^1H\}$ NMR ($CDCl_3$): $\delta = 34.45$ ppm (br s).

trans-*[Rh(**1**$^{-}$·**2**$^{+}$)Cl(CO)]*: Several experiments were conducted to determine the structure of this compound. The crystals are sensitive and tend to lose solvent molecules quickly, which results in the collapse of the crystal. The best quality crystals were obtained in the following manner: Ionic assembly **1**$^{-}$·**2**$^{+}$ (26 mg, 0.042 mmol) and [Rh($CO)_2$Cl]$_2$ (7.8 mg, 0.02 mmol) were stirred in CH_3CN (5 mL). The product precipitated immediately. Therefore, THF (1 mL) was added to obtain a homogeneous solution. The next day yellow crystals of *trans*-[Rh(**1**$^{-}$·**2**$^{+}$)(CO)Cl] were deposited on the wall of the vial.

Acknowledgements

BASF is kindly acknowledged for financial support of this work. Z.F. acknowledges the Spanish MEC for a "Ramon y Cajal" contract.

[1] a) M. T. Reetz, T. Sell, A. Meiswinkel, G. Mehler, *Angew. Chem.* **2003**, *115*, 814–817; *Angew. Chem. Int. Ed.* **2003**, *42*, 790–793; b) M. T. Reetz, G. Mehler, *Tetrahedron Lett.* **2003**, *44*, 4593–4596; c) D. Peña, A. J. Minnaard, J. A. F. Boogers, A. H. M. de Vries, J. G. de Vries, B. L. Feringa, *Org. Biomol. Chem.* **2003**, *1*, 1087–1089; d) M. T. Reetz, X. Li, *Tetrahedron* **2004**, *60*, 9709–9714; e) M. T. Reetz, G. Mehler, A. Meiswinkel, T. Sell, *Tetrahedron: Asymmetry* **2004**, *15*, 2165–2167; f) M. T. Reetz, Y. Fu, A. Meiswinkel, *Angew. Chem.* **2006**, *118*, 1440–1443; *Angew. Chem. Int. Ed.* **2006**, *45*, 1412–1415.

[2] A. Duursma, R. Hoen, J. Schuppan, R. Hulst, A. J. Minnaard, B. L. Feringa, *Org. Lett.* **2003**, *5*, 3111–3113.

[3] M. T. Reetz, X. Li, *Angew. Chem.* **2005**, *117*, 3019–3021; *Angew. Chem. Int. Ed.* **2005**, *44*, 2962–2964.

[4] a) V. F. Slagt, M. Röder, P. C. J. Kamer, P. W. N. M. van Leeuwen, J. N. H. Reek, *J. Am. Chem. Soc.* **2004**, *126*, 4056–4057; b) J. N. H. Reek, M. Röder, P. E. Goudriaan, P. C. J. Kamer, P. W. N. M. van Leeuwen, V. F. Slagt, *J. Organomet. Chem.* **2005**, *690*, 4505–4516; c) X.-J. Jiang, L. Lefort, P. E. Goudriaan, A. H. M. de Vries, P. W. N. M. van Leeuwen, J. G. de Vries, J. N. H. Reek, *Angew. Chem.* **2006**, *118*, 1245–1249; *Angew. Chem. Int. Ed.* **2006**, *45*, 1223–1227.

[5] a) B. Breit, W. Sache, *Angew. Chem.* **2005**, *117*, 4401–4404; *Angew. Chem. Int. Ed.* **2005**, *44*, 1640–1643; b) M. Weis, C. Waloch, W. Seiche, B. Breit, *J. Am. Chem. Soc.* **2006**, *128*, 4188–4189.

[6] a) For a recent computational study on the factors controlling the relative stabilities of *cis*- and *trans*-PtX_2L_2 isomers, see: J. N. Harvey, K. M. Heslop, A. G. Orpen, P. G. Pringle, *Chem. Commun.* **2003**, 278–279; b) M. R. Eberhard, K. M. Heslop, A. G. Orpen, P. G. Pringle, *Organometallics* **2005**, *24*, 335–337.

[7] C. A. Hunter, *Angew. Chem.* **2004**, *116*, 5424–5439; *Angew. Chem. Int. Ed.* **2004**, *43*, 5310–5324.

[8] Crystal data for *cis*-[Pt(**2**)(**3**)Cl_2] at 100 K: $C_{39}H_{40}Cl_3N_3O_1P_2Pt_1$; 930.12 g mol^{-1}; triclinic; $P2_1/c$; $a = 10.3025(16)$, $b = 24.451(4)$, $c = 15.062(2)$ Å; $\beta = 97.516(5)°$; $V = 3761.5(10)$ Å^3; $Z = 4$; $\rho_{calcd} = 1.642$ Mg m^{-3}; $R_1 = 0.0376$ (0.0462); $wR_2 = 0.0868$ (0.0902); for 17762 reflections with $I > 2\sigma(I)$ (for 20381 reflections [R_{int}: 0.0298] with a total of 71782 measured reflections); goodness-of-fit on $F^2 = 1.244$; largest diff. peak (hole) = 2.338 (−1.894) e Å^{-3}.

[9] The ^{31}P NMR spectroscopic characteristics of *cis*-[Pt(**1**$^{-}$·**2**$^{+}$)Cl_2] vary slightly with the solvent. Representative ^{31}P NMR ($CDCl_3$/CD_3OD, v/v = 5): $\delta = 15.50$ (d, J(P,P) = 15.9 Hz, ^1J(Pt,P) = 3607 Hz), 20.87 ppm (d, J(P,P) = 15.9 Hz, ^1J(Pt,P) = 3771 Hz).

[10] The ^{31}P NMR spectroscopic characteristics of *cis*-[Pt(**1**$^{-}$)$_2Cl_2$]·*cis*-[Pt(**2**$^{+}$)$_2Cl_2$] vary slightly with the solvent. The resonances of the anionic and cationic complex overlap in several solvent systems. Representative ^{31}P NMR (CD_3OD/DMF, v/v = 1): $\delta = 17.18$ (s, J-(Pt,P) = 3686 Hz), 17.36 ppm (s, J(Pt,P) = 3690 Hz).

[11] Crystal data for *cis*-[Pt(**6**)$_2Cl_2$] at 100 K: $C_{38}H_{34}Cl_2O_2P_2Pt_1 \cdot {}^1/_2C_1H_1Cl_3$; 910.27 g mol^{-1}; triclinic; $P\bar{1}$; $a = 11.1876(14)$, $b = 12.1238(15)$, $c = 16.2261(19)$ Å; $\alpha = 91.801(3)$, $\beta = 107.201(3)$, $\gamma = 113.421(3)°$; $V = 1901.1(4)$ Å^3; $Z = 2$; $\rho_{calcd} = 1.590$ Mg m^{-3}; $R_1 = 0.0582$ (0.0650); $wR_2 = 0.01589$ (0.1646); for 12262 reflections with $I > 2\sigma(I)$ (for 13546 reflections [R_{int}: 0.0343] with a total of 31412 measured reflections); goodness-of-fit on $F^2 = 1.129$; largest diff. peak (hole) = 4.640 (−3.275) e Å^{-3}. Crystal data for *cis*-[Pt(**1**$^{-}$·**2**$^{+}$)Cl_2] at 100 K: $C_{41}H_{41}Cl_2N_3O_4P_2Pt_1S_1$; 999.76 g mol^{-1}; triclinic; $P\bar{1}$; $a = 10.1891(11)$, $b = 12.6860(13)$, $c = 15.7962(16)$ Å; $\alpha = 81.116(2)$, $\beta = 84.807(3)$, $\gamma = 73.142(3)°$; $V = 1928.4(3)$ Å^3; $Z = 2$; $\rho_{calcd} = 1.772$ Mg m^{-3}; $R_1 = 0.0360$ (0.0455); $wR_2 = 0.0901$ (0.1001); for 12205 reflections with $I > 2\sigma(I)$ (for 13782 reflections [R_{int}: 0.0399] with a total of 32624 measured reflections); goodness-of-fit on $F^2 = 1.040$; largest diff. peak (hole) = 5.649 (−4.395) e Å^{-3}.

[12] Preliminary MM2 analysis of **1**$^{-}$·**2**$^{+}$ coordinated to a nonconfigured metal shows that the natural bite angle of the ionically assembled phosphane is larger than 150°, and the *trans*-coordination mode is more favorable than the *cis* geometry. However, the small energy difference (6 kcal mol^{-1}) between the *trans* and *cis* structures indicates that other factors, such as the *trans* influence of other ligands, might determine the geometry of the transition-metal complexes of **1**$^{-}$·**2**$^{+}$.

[13] Crystal data for *trans*-[Pd(**4**)$_2$(CH_3)Cl] at 100 K: $C_{61}H_{51}O_2P_4Pd_1 \cdot C_1H_2Cl_2$; 1124.21 g mol^{-1}; triclinic; $P\bar{1}$; $a = 9.4561(7)$, $b = 15.6232(12)$, $c = 18.7685(14)$; $\alpha = 76.543(2)$, $\beta = 77.078(2)$, $\gamma = 76.452(2)°$; $V = 2579.3(3)$ Å^3; $Z = 2$; $\rho_{calcd} = 1.448$ Mg m^{-3}; $R_1 = 0.0434$ (0.0494); $wR_2 = 0.1125$ (0.1168); for 21238 reflections with $I > 2\sigma(I)$ (for 23758 reflections [R_{int}: 0.0385] with a total of 52460 measured reflections); goodness-of-fit on $F^2 = 1.064$; largest diff. peak (hole) = 2.209 (-2.041) e Å^{-3}. Crystal data for *trans*-[Pd(**1**$^{-}$·**2**$^{+}$)(CH_3)Cl] at 100 K: $C_{37}H_{34}Cl_1N_1O_3P_2Pd_1S_1$, 776.50 g mol^{-1}; rhombohedral; $R\bar{3}$; $a = 20.9955(5)$ Å; $\alpha = 103.68(2)°$; $V = 8308.3(3)$ Å^3; $Z = 6$; $\rho_{calcd} = 0.931$ Mg m^{-3}; $R_1 = 0.0668$ (0.0956); $wR_2 = 0.1901$ (0.2086); for 10932 reflections with $I > 2\sigma(I)$ (for 16928 reflections [R_{int}: 0.0696] with a total of 108109 measured reflections); goodness-of-fit on $F^2 = 1.015$; largest diff. peak (hole) = 2.274 (−0.712) e Å^{-3}. This structure shows pseudosymmetry. Refinement in $Pna2_1$ led to $R_1 = 0.1013$ with negative atomic displacement parameters owing to correlation effects. Compound **3b** includes highly disordered chloroform molecules in the crystal structure and was treated with Squeeze (Platon) to avoid modeling the disordered molecules; A. L. Spek, *Acta Crystallogr.* **1990**, *A46*, C34; A. L. Spek, Platon: A Multipurpose Crystallographic Tool, University of Utrecht, Utrecht (The Netherlands), **2003**.

[14] Crystal data for *trans*-[Rh(**1**$^{-}$·**2**$^{+}$)(CO)Cl] at 100 K: $C_{37}H_{31}Cl_1N_1O_4P_2Rh_1S_1 \cdot 1.42\ C_2N_1H_3 \cdot 0.75\ H_2O$ (some of the hydrogen atoms could not be localized); 855.81 g mol^{-1}; rhombohedral; $R\bar{3}$; $a = 32.4705(11)$, $c = 27.6370(18)$ Å; $V = 25235(2)$ Å^3; $Z = 18$; $\rho_{calcd} = 1.014$ Mg m^{-3}; $R_1 = 0.0834$ (0.1364); $wR2 = 0.2441$ (0.3037); for 5330 reflections with $I > 2\sigma(I)$ (for 8090 reflections [R_{int}: 0.0593] with a total of 48451 measured reflections); goodness-of-fit on $F^2 = 1.122$; largest diff. peak (hole) = 1.388 (−909) e Å^{-3}.

[15] R. E. Rülke, J. M. Ernsting, A. L. Spek, C. J. Elsevier, P. W. N. M. van Leeuwen, K. Vrieze, *Inorg. Chem.* **1993**, *32*, 5769–5778.

[16] O. Herd, A. Hessler, M. Hingst, M. Tepper, O. Stelzer, *J. Organomet. Chem.* **1996**, *522*, 69–76.

[17] D. Wittenberg, H. Gilman, *J. Org. Chem.* **1958**, *23*, 1063–1065.

[18] a) P. J. Roman, Jr., D. P. Paterniti, R. F. See, M. R. Churchill, J. D. Atwood, *Organometallics* **1997**, *16*, 1484–1490; b) F. Joó, J. Kovács,

Á. Kathó, A. C. Bényei, T. Decuir, D. J. Darensbourg in *Inorg. Synth., Vol. 32* (Ed.: M. Y. Darensbourg), Wiley, **1998**, pp. 1–8.
[19] A. Hessler, O. Stelzer, H. Dibowski, K. Worm, F. P. Schmidtchen, *J. Org. Chem.* **1997**, *62*, 2362–2369.
[20] A. Buhling, P. C. J. Kamer, P. W. N. M. van Leeuwen, *J. Mol. Catal. A: Chem.* **1995**, *98*, 69–80.

Received: October 9, 2006
Published online: February 9, 2007

